

Wind turbine foundation deburial sensors based on induction-heated ceramic patches

Marcus Perry¹, Mohamed Saafi², Grzegorz Fusiek³, and Pawel Niewczas³

¹ Civil and Environmental Engineering, University of Strathclyde, Glasgow, United Kingdom

² Department of Engineering, Lancaster University, Lancaster, United Kingdom

³ Electronic and Electrical Engineering, University of Strathclyde, Glasgow, United Kingdom

ABSTRACT: The deburial and scouring of concrete wind turbine and bridge foundations presents a risk to structural stability and safety. In this work, we present a novel, ceramic temperature-sensing patch which can detect whether sections of a foundation are buried or exposed to air. The sensor patches, applied to concrete specimens, were fabricated by loading a geopolymer with 0 - 60 wt% ground magnetite. The magnetite content allowed the patches to be heated using an induction coil, while temperature profiles were monitored via changes in patch electrical impedance. Sensor patches were left uncoated, or were coated in surface-water, soil and sand. Each material provided a unique thermal signature which, with simple signal processing, could be used to reliably detect whether the patch was buried.

1 INTRODUCTION

Foundation deburial and scouring can degrade the stability of any large civil structure. Structures subjected to large dynamic loads or changing water levels, such as wind turbines and bridges, are particularly affected, Whitehouse et al (2011). Traditional automated scour monitoring methods and instrumentation are often expensive to install and maintain, so there is keen interest in developing new deburial monitoring systems.

Several methods have been proposed for deburial detection, including solutions based on fibre optics and micro-electromechanical system (MEMS) devices, Pendergast et al (2014). Unfortunately, the technical challenge of providing robust packaging for fibre and MEMS sensors can present a barrier to their widespread use, Miller et al (2014), Jiang et al (2007).

Geopolymer binders are a novel class of chemically stable, low shrinkage piezoresistive materials, which are highly suited to civil applications. Unintrusive and easy to apply, geopolymer binders provide excellent adhesion to concrete structures, Pacheco-Torgal et al (2008). Once cured, the binders form a tough ceramic-like resin that can be used to detect environmental parameters via changes in electrical impedance, Saafi et al (2014).

In this preliminary work, geopolymer binders are doped with a ferromagnetic mineral and then applied to concrete surfaces. The doping allows the patches to be heated using an induction coil, while the electrical impedance of the patches is interrogated to monitor patch temperature during heating and cooling. Thermal decay signatures are then used to detect whether the sensor is surrounded by air, soil, sand, or a mixture of these materials. It is proposed that these geopolymer sensor patches may provide a new method of detecting deburial of wind turbine foundations.

2 THEORY OF OPERATION

2.1 Geopolymer binders

Adhesive geopolymer gels can be created by mixing fly ash with an alkaline activator. When the gel is exposed to elevated temperatures, it cures over several hours to form a solid, ceramic-like binder. On the microscale, geopolymers are amorphous materials, comprised of a matrix of long, cross-linked chains of tetrahedral AlO_4 and SiO_4 units, Hanjitsuwan et al (2011). Free alkali ions, such as Na^+ , reside within this matrix to balance its electrical charge. These residual ions act as charge carriers, allowing geopolymers to behave as fast ionic conductors, with conductivities of order 10^{-6} S/cm, Cui et al (2008).

When an alternating current, I , is applied across a geopolymer, the measured voltage, V , is dependent on the specimen's impedance, Z :

$$\frac{V}{I} = Z = \frac{L}{\sigma A} \quad (1)$$

Here, σ and L are the conductivity and length of the geopolymer sample, while A is the contact area between the geopolymer and the electrodes. If it is assumed that the contact area remains reasonably constant, then partial differentiation of (1) reveals the temperature, T , dependence of the impedance:

$$\frac{1}{Z} \frac{\partial Z}{\partial T} = \alpha_L - \frac{1}{\sigma} \frac{\partial \sigma}{\partial T} \quad (2)$$

where $\alpha_L = (1/L)(\partial L/\partial T) \approx 10^{-6} \text{ }^\circ\text{C}^{-1}$, is the geopolymer's coefficient of thermal expansion (Davidovits 2008). The dependence of ionic conductivity on temperature is governed by the Arrhenius equation, parameterised by a constant B , Daniel et al (2011):

$$\sigma \propto e^{-B/(T-T_g)} \quad (3)$$

where $T_g \approx 800$ K is the geopolymer glass transition temperature, Pan et al (2010). The parameter B is proportional to the activation energy of the alkali ions in the geopolymer, and typically takes a value $\sim 10^4$. Note that below T_g , geopolymer conductivity increases with temperature because the alkali charge carriers become more mobile as the sample is heated. Differentiation of equation (3) and substitution into (2) shows that the temperature sensitivity of the impedance takes the form:

$$\frac{\Delta Z}{Z} = \left(\alpha_L - \frac{B}{(T - T_g)^2} \right) \Delta T \quad (4)$$

where $B/(T-T_g)^2 \gg \alpha_L$. Below T_g , fractional shifts in the measured impedance take unique values. If the geopolymer patch remains close to room temperature, then $T_g \gg T$, and equation (4) is approximately linear:

$$\frac{\Delta Z}{Z} \approx \left(\frac{B}{T_g^2} \right) \Delta T \quad (5)$$

Characterisation of this equation allows geopolymer patches to be used as thermometers

2.2 Induction heating

Alternating the current within an induction coil sets up a local, temporally changing magnetic field. This can initiate Eddy currents at the surfaces of nearby conductors, resulting in Joule heating. While geopolymers may experience some Joule heating, their electrical conductivities are $\sim 10^{12}$ times lower than most metals, so the Eddy currents generated are small.

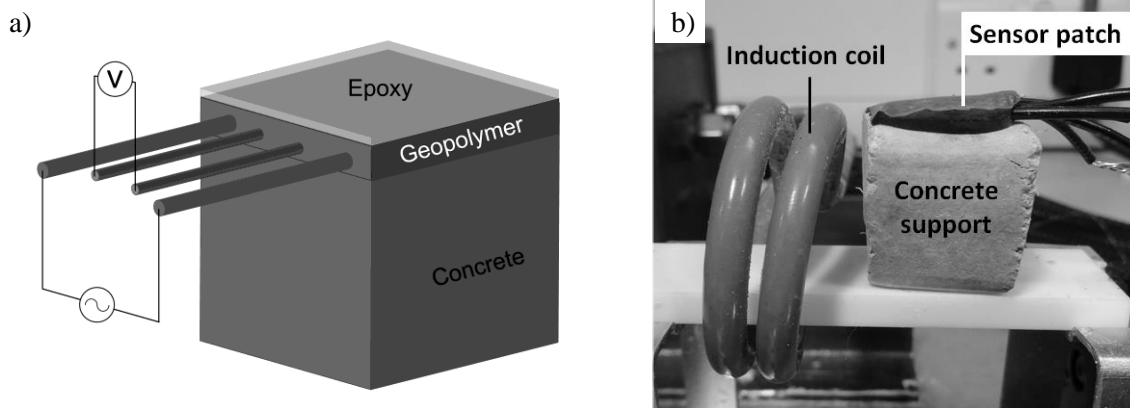
To enhance heating, geopolymer gels may be doped with ferromagnetic materials prior to curing. Ferromagnets possess an inherent magnetisation, designated by the vector \mathbf{M} . Application of the induction coil's external field, \mathbf{H} , causes the magnetic domains within the ferromagnet to expand and contract along the axis of \mathbf{M} . During one cycle of the H-field, the friction produced by this movement generates additional heat.

3 SENSOR MANUFACTURE AND TESTING

3.1 Overview

The configuration of the geopolymer patch sensor is shown in Figure 1a. A magnetite-doped geopolymer sensing patch is applied to the surface of a small concrete cube (each side approximately 3 cm) and protected with a thin layer of epoxy. Four electrical probes are embedded into the geopolymer layer. An alternating current, I , is applied across the two outer probes using a current source, while the voltage, V , is measured over the two inner probes. Impedance, Z , is then calculated using equation (1). Separation of the electrodes allows for more accurate impedance monitoring as it reduces contact and lead resistances.

Figure 1, The configuration of the geopolymer patch sensor, shown in a), and the induction heating set up, shown in b).



The patch sensor was left uncovered in air or covered with surface water, dry sand, wet sand or wet soil. The instrumented concrete block was then heated by a two-turn induction coil, as shown in Figure 1b. The current within the coil was driven at 100 – 200 A amplitude and 350 kHz frequency for 15-20 seconds.

For initial characterisation, patches of varying magnetite content were heated in air for 20 seconds while sensor impedance was monitored. Temperature measurements from a fibre Bragg grating thermometer were used to verify that impedance shifts were indeed a result of

geopolymer patch heating. Finally, a patch with 35 wt% magnetite content was sequentially tested while uncovered and while covered in surface water, dry sand, wet sand, or wet soil. Impedances were monitored for each case during 15 seconds of induction heating and ~80 seconds of cooling.

3.2 Manufacturing method

The geopolymer gel was fabricated by combining 72 wt% low-calcium, class-F fly ash, with 20 wt% sodium silicate solution (Na_2SiO_3 , with 29.4 wt% SiO_2 and 14.7 wt% NaO_2 , in water) and 8 wt% of 10 M sodium hydroxide solution.

Batches of geopolymer gel, each 2 – 3 grams, were mixed with varying quantities of crushed magnetite – a ferromagnetic mineral containing iron oxides. Magnetite contents in each batch varied from 0 – 60 % by weight. Each doped geopolymer gel batch was applied to the surface of a separate concrete cube, prior to curing in an oven for 3 days at 40 °C. After curing, a thin layer of epoxy was applied over the patches to protect them from mechanical abrasion and changing chemical contamination, as these factors may lead to spurious impedance signals.

3.3 Interrogation

Alternating currents of 30 – 80 μA amplitude were applied across the outer-probes of the sensor, while the voltage over the inner probes was measured using a data acquisition card. The typical voltage noise was 2 mV and the interrogation rate was ~10 kHz. High-frequency alternating currents at 1 kHz frequency were used during impedance monitoring as this reduces the effects of capacitance and false polarisation potentials at the sensor electrodes, Saiprasad et al (2011).

4 RESULTS

4.1 Initial characterisation

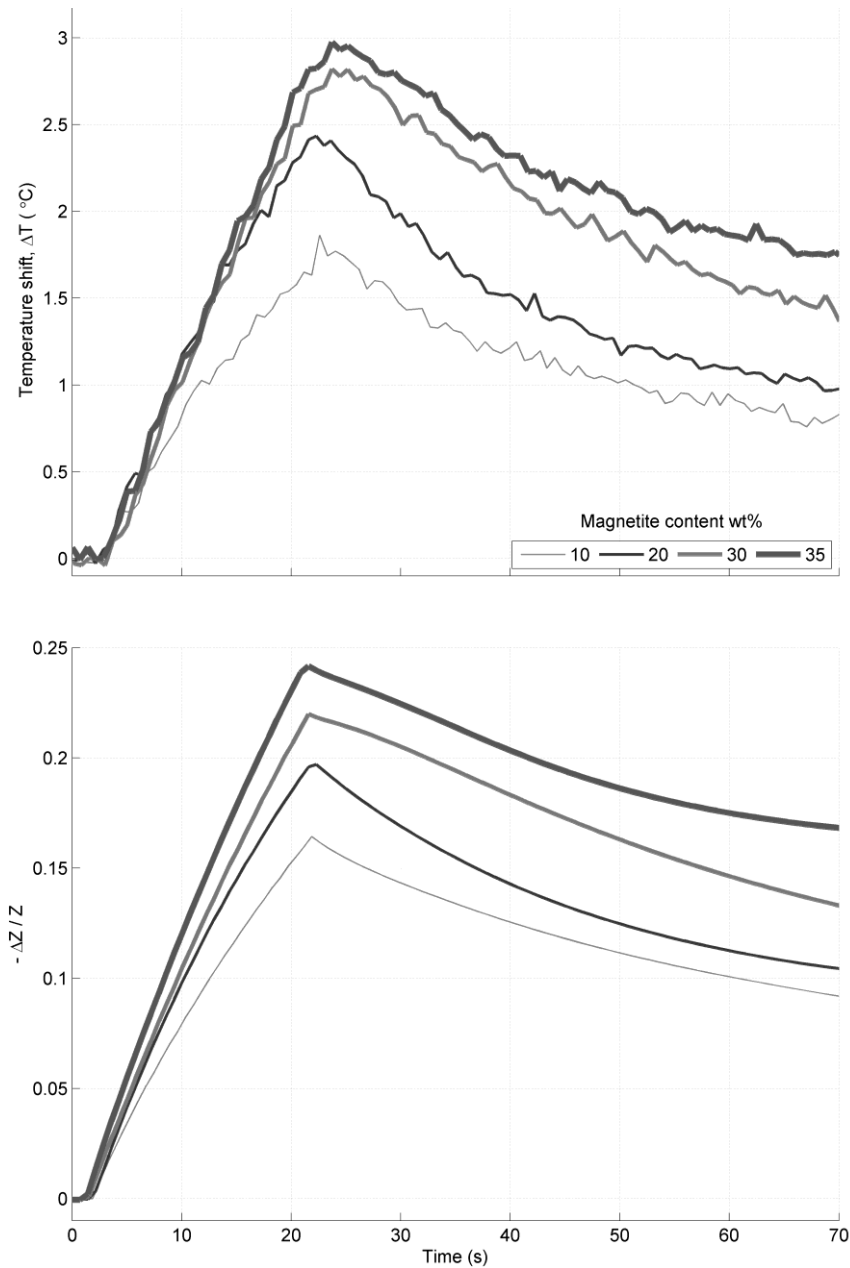
Figure 2 shows the evolution of patch temperature (as measured by the fibre gauge) and its electrical impedance during 20 seconds of induction heating and one minute of cooling. Profiles for magnetite contents of $W = 10, 20, 30$ and 35 wt% are shown. For $W < 30$ wt%, the maximum temperatures achieved are approximately linear with magnetite content. Beyond this, temperature saturation occurs as the induction heating rate cannot overcome heat losses.

The temperature and impedance profiles match, which confirms that the impedance is providing a measurement of heating and cooling. As the geopolymer sensor is more sensitive to temperature than the fibre gauge, the impedance signal provides a low-noise, high resolution measurement.

The peaks in temperature and impedance shifts from Figure 2 are plotted against each other in Figure 3. This is a graphical representation of equation (5), and so the parameter $B = 5 \times 10^4$ can be estimated from the slope of the linear fit. This is of the same order (10^4) as that suggested by underlying ionic conductor theory.

Note that, while the results are not presented here, sensors with magnetite contents as high as 60 wt% were briefly tested. The higher contents yielded little or no improvement to induction heating. Furthermore, as with any cementitious substance, as more aggregate (magnetite) was added to the geopolymer, its flow and adhesion decreased. This decreased the robustness of the patches, so geopolymer gels with 35 wt% magnetite were used for the remainder of this work.

Figure 2, Temperature and impedance evolution of doped magnetite geopolymer specimens during 20 seconds of induction heating.



4.2 Deburial sensing

The 35 wt% patch sensor was left uncovered or covered in water, soil or sand and then induction heated for 15 seconds. The impedance profiles for the various materials tested are shown in Figure 4. Note that two separate cases for air are provided to demonstrate sensor repeatability.

While there are minor differences in the temperature rise portions of the graphs, the temperature decays provide a more distinct signature for each material. Temperature decays are slower for

air and sand due to their lower thermal conductivities (<1 W/m.K). Wet soil and wet sand have much higher thermal conductivities (1-4 W/m.K) and so provide the most rapid temperature decays.

Figure 3, Relationship between maximum geopolymer temperature and impedance shift. Magnetite contents (wt%) are labelled.

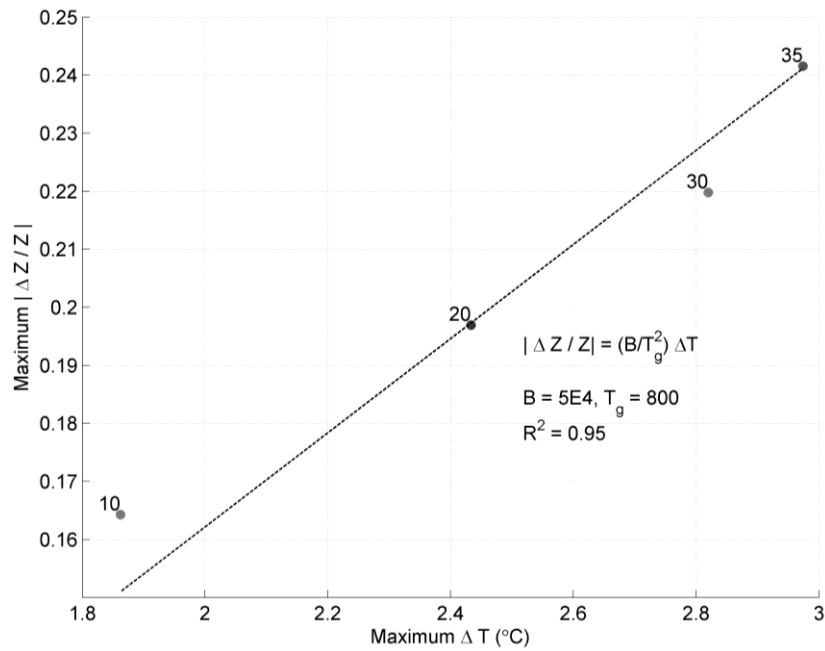
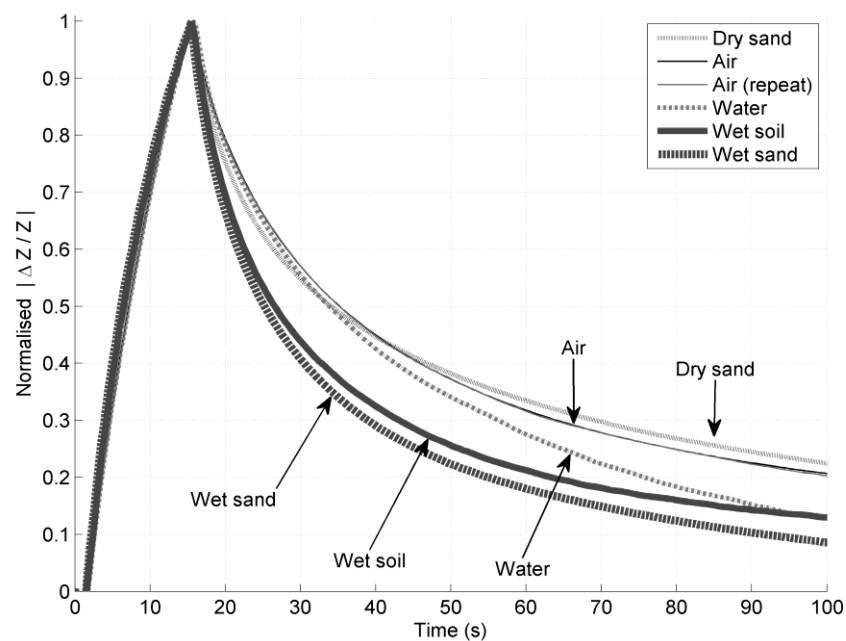


Figure 4, Patch (35 wt% magnetite) response during 15 seconds of induction heating. The sensor was covered in dry sand, nothing (air), water, wet soil and wet sand. The impedance response has been normalised by its maximum value.



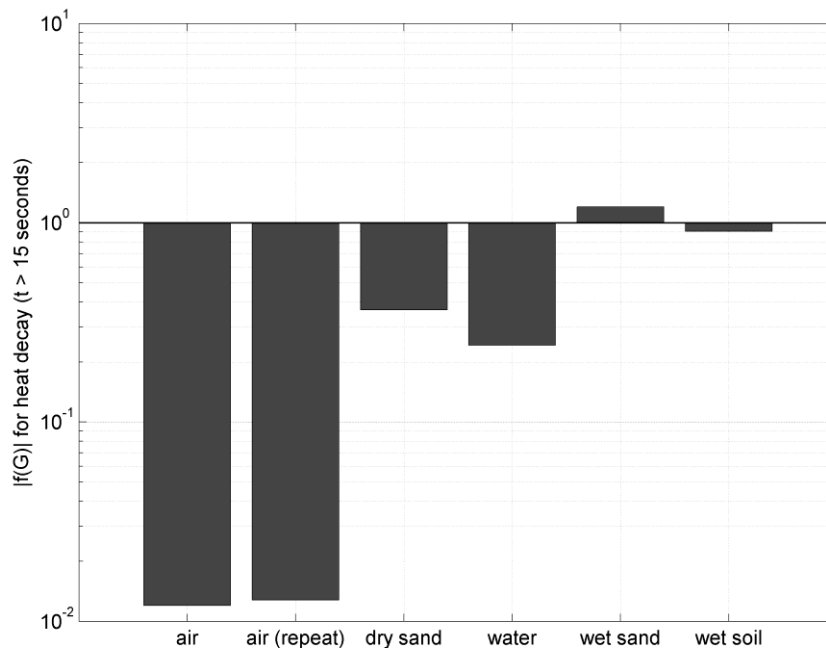
In this work, a simple algorithm was written to allow software to distinguish between the impedance-shift signatures for each material. The line labelled *air* in Figure 4 provides a set of reference impedance-shift values. These are denoted Air_i , for $i = 1 \dots N$. Any other line, such as *dry sand*, can be denoted by a different set, G_i . The difference between G_i and Air_i is calculated on a point-by-point basis, and the difference is then integrated numerically:

$$f(G) = \frac{\Delta t}{2} \sum_{i=1}^N (G_i - Air_i) + (G_{i+1} - Air_{i+1}) \quad (6)$$

where Δt is the time interval between measurement points.

Values for $|f(G)|$ for each of the materials tested are provided in Figure 5. Each of the materials is clearly distinguishable from air, so if the sensor is able to detect deburial. There are limitations to the approach, however. While water and dry sand signatures are clearly distinguishable in Figure 4, the difference is less obvious in Figure 5. Distinguishing between these, and a wider variety of materials at different ambient temperatures in real applications, may require more sophisticated machine learning approaches.

Figure 5, Values of $|f(G)|$ for the impedance decay of each line from Figure 4.



5 CONCLUSIONS

Concrete foundation deburial sensor patches have been fabricated by doping geopolymer gels with ground magnetite. When the geopolymer gel's magnetite content was less than 35 wt%, it retained its adhesion and flow characteristics, allowing it to be painted on to concrete surfaces prior to curing. Once cured, the magnetite doping allowed the patches to be heated by up to 3 °C within 20 seconds using a 100 A induction coil. Temperature changes in the patch were monitored via changes in its electrical impedance. In this preliminary work, sensor patches were able to distinguish between the presence of air, surface water, dry sand, wet sand and wet soil,

as each material provided a unique thermal signature. Crucially this allows the sensor to detect whether it is buried. With further development, these sensors may be used to monitor scouring of wind turbine foundations, deep sea cables and bridges.

6 REFERENCES

- Daniel, C. and Besenhard, J.O. 2011. *Handbook of Battery Materials 2nd Edition*. New York: John Wiley & Sons, Inc.
- Cui, X., Zheng, G, Han, Y., Su, F. and Zhou, J. 2008. A study on electrical conductivity of chemosynthetic Al₂O₃-2SiO₂ geopolymer materials. *Journal of Power Sources*, 184(2):652-656.
- Davidovits, J. *Geopolymer Chemistry and Applications 2nd Edition*. Saint-Quentin: Institut Geopolymere.
- Hanjitsuwan, S., Chindapasirt, P., and Pimraksa, K. 2011. Electrical conductivity and dielectric property of fly ash geopolymer pastes. *International Journal of Minerals*, 18(1): 94-99.
- Hill, K.O. and Meltz, G. 1997. Fiber Bragg grating technology fundamentals and overview. *Journal of Lightwave technology*, 15(8): 1263-1276.
- Jiang, L. and Spearing, S.M., 2007. A reassessment of materials issues in microelectromechanical systems (MEMS). *Journal of the Indian Institute of Science*, 87(3): 363-385.
- Miller, J.W. and Mendez, A. 2014, Fiber Bragg Grating Sensors: Market Overview and New Perspectives. *Fiber Bragg Grating Sensors: Recent Advancements, Industrial Applications and Market Exploitation*, 8: 313-320.
- Pacheco-Torgal, F., Castro-Gomes, J. and Jalali, S. 2008. Alkali-activated binders: A review. *Construction and Building Materials*, 22(7): 1305-1322.
- Pan, Z. and Sanjayan, J.G. 2010. Stress-strain behaviour and abrupt loss of stiffness of geopolymer at elevated temperatures. *Cement and Concrete Composites*, 32(9): 657-664.
- Pendergast, L.J. and Gavin, K 2014. A review of bridge scour monitoring techniques. *Journal of Rock Mechanics and Geotechnical Engineering*, 6(2): 138-149.
- Saafi, M., Tang, L., Fung, J., Rahman, M., Sillars, F., Liggart J. and Zhou, X. 2014. Graphene/fly ash geopolymeric composites as self-sensing structural materials. *Smart Materials and Structures*, 23(6).
- Saiprasad V. and Allouche, E.N. 2011. Experimental evaluation of electrical conductivity of carbon fiber reinforced fly-ash based geopolymer. *Smart Structures and Systems*, 7(1): 27-40.
- Whitehouse, R.J.S, Harris, J.M., Rees, J. 2011. The nature of scour development and scour protection at offshore windfarm foundations, *Marine Pollution Bulletin*, 62(1): 73-88.